Development 134, 4095-4106 (2007) doi:10.1242/dev.010272

Lrp6 is required for convergent extension during *Xenopus* gastrulation

Emilios Tahinci[1], Curtis A. Thorne[1], Jeffrey L. Franklin[1,2], Adrian Salic[3], Kelly M. Christian[1], Laura A. Lee[1], Robert J. Coffey[1,2] and Ethan Lee[1,*]

Wnt signaling regulates β-catenin-mediated gene transcription and planar cell polarity (PCP). The Wnt co-receptor, Lrp6, is required for signaling along the β-catenin arm. We show that Lrp6 downregulation (by morpholino injection) or overexpression in *Xenopus* embryos disrupts convergent extension, a hallmark feature of Wnt/PCP components. In embryos with decreased Lrp6 levels, cells of the dorsal marginal zone (DMZ), which undergoes extensive cellular rearrangements during gastrulation, exhibit decreased length:width ratios, decreased migration, and increased numbers of transient cytoplasmic protrusions. We show that Lrp6 opposes Wnt11 activity and localizes to the posterior edge of migrating DMZ cells and that Lrp6 downregulation enhances cortical and nuclear localization of Dsh and phospho-JNK, respectively. Taken together, these data suggest that Lrp6 inhibits Wnt/PCP signaling. Finally, we identify the region of the Lrp6 protein with Wnt/PCP activity to a stretch of 36 amino acids, distinct from regions required for Wnt/β-catenin signaling. We propose a model in which Lrp6 plays a critical role in the switch from Wnt/PCP to Wnt/β-catenin signaling.

KEY WORDS: Lrp6, Wnt, Planar cell polarity, Convergent extension, Gastrulation, *Xenopus*

INTRODUCTION

Studies have shown the existence of at least two Wnt pathways that play critical roles in early embryonic development: Wnt/β-catenin ('canonical') and Wnt/PCP (planar cell polarity or 'noncanonical') signaling. Of the two, the best characterized is the Wnt/β-catenin pathway (reviewed by Clevers, 2006). In the absence of a Wnt signal, cytoplasmic β-catenin is normally maintained at low levels due to its degradation by a complex consisting of Axin, the tumor suppressor APC (adenomatous polyposis coli), and the kinases CKIα and GSK3. Activation of Wnt/β-catenin signaling occurs upon binding of Wnt ligands to members of the Frizzled (Fz) and low-density lipoprotein receptor-related protein family of receptors (Tamai et al., 2000; Wehrli et al., 2000). Wnt binding initiates a series of events resulting in β-catenin stabilization and consequent activation of gene transcription by binding of β-catenin to members of the TCF/LEF family of transcription factors.

Wnt/PCP signaling controls convergent-extension movements of the axial and paraxial mesoderm and neural ectoderm during embryonic development in *Xenopus*, zebrafish and mice (Jones and Chen, 2007). In *Xenopus* embryos, the Wnt/PCP pathway affects cell morphology and motility largely through its modulation of the actin cytoskeleton. Cells acquire distinct polar morphologies that promote directed migration and intercalation during the morphogenetic movements of gastrulation and neurulation. Although numerous genes that regulate Wnt/PCP signaling have been identified, mechanisms by which the signal is transduced are not well understood. Assembly of the actin cytoskeleton as a consequence of Wnt/PCP signaling is thought to occur via cortical recruitment of Dishevelled (Dsh; also known as Dvl – Xenbase) and activation of Jun-N-terminal kinase (JNK) and the Rho family of GTPases (Habas et al., 2001; Yamanaka et al., 2002).

[1]Department of Cell and Developmental Biology and [2]Department of Medicine, Vanderbilt University Medical Center, Nashville, TN 37232, USA. [3]Department of Cell Biology, Harvard Medical School, Boston, MA 02115, USA.

*Author for correspondence (e-mail: ethan.lee@vanderbilt.edu)

Accepted 5 September 2007

Lrp6 has been shown to play a critical role in activating Wnt/β-catenin signaling. Its intracellular domain contains five PPP(S/T)P motifs, each of which is phosphorylated upon Wnt stimulation (Davidson et al., 2005; Zeng et al., 2005). Each of the five PPP(S/T)P motifs of Lrp6, when phosphorylated, can bind to Axin and, through an as yet undefined mechanism, inhibit β-catenin degradation (Tamai et al., 2004). In the current model of Wnt signaling, Lrp6 signals exclusively in a β-catenin-dependent manner (Tamai et al., 2000; Wehrli et al., 2000). Recently, Dkk1, a secreted Wnt/β-catenin antagonist that binds Lrp6, was shown to regulate convergent-extension movements in zebrafish via activation of Wnt/PCP signaling (Caneparo et al., 2007).

Our studies indicate that Lrp6, a previously characterized core Wnt/β-catenin component, is an essential regulator of convergent-extension movements in *Xenopus* embryos via its inhibition of Wnt/PCP signaling. Furthermore, we show that Lrp6 is asymmetrically distributed in mesodermal cells that participate in convergent extension, suggesting a role for Lrp6 in the establishment and maintenance of cell polarity during embryogenesis.

MATERIALS AND METHODS

Embryo injections, dissections and staining

Xenopus embryos were fertilized in vitro, dejellied, and cultured as previously described (Peng, 1991). Embryos were staged according to Nieuwkoop and Faber (Nieuwkoop and Faber, 1994). For microinjections, embryos were kept in 3% Ficoll in 0.2× Marc's modified Ringer's (MMR) medium and fixed at stage 26 for analysis. In vitro-transcribed, capped mRNA was synthesized using the mMessage mMachine Kit (Ambion, Austin, TX, USA). Lrp6MO was from Gene Tools LLC (Philomath, OR, USA). Detection of notochord with monoclonal antibody Tor70 (Kushner, 1984) was performed as described previously (Lane and Keller, 1997).

Keller sandwiches of uniform width and length were prepared from dorsal marginal zone (DMZ) explants at stage 10+ (Keller and Danilchik, 1988) and cultured in 1× DFA medium (Sater et al., 1993) until stage 18. To determine explant length-to-width ratios, the longest axis of each explant was divided by its widest perpendicular aspect (short axis). Animal pole ectodermal explants (animal caps) were dissected at stage 9 and cultured in 75% MMR in the presence of 10 ng/ml activin (R&D Systems, Minneapolis, MN, USA) until stage 20 when elongation was assessed. At least 28 caps were assessed for each set of injections.

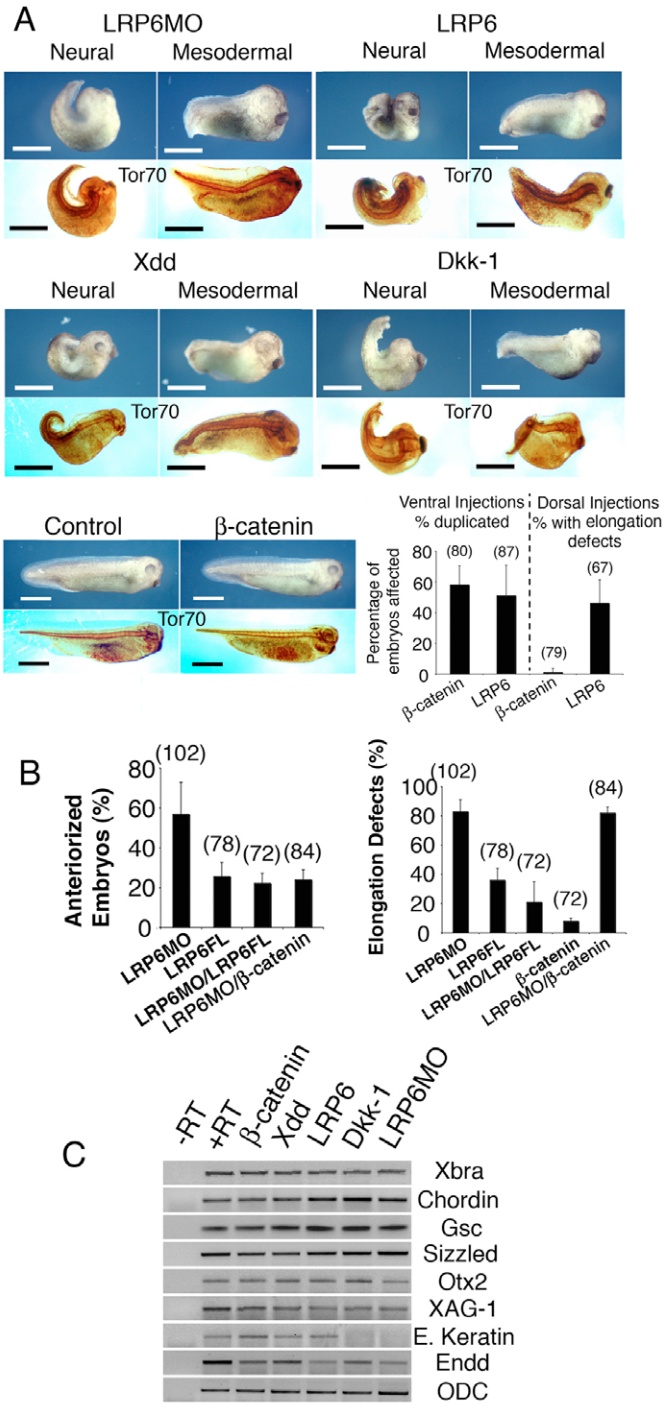

Fig. 1. Loss or gain of Lrp6 function inhibits convergent extension without affecting tissue patterning. (**A**) Dorsal injections of Lrp6 morpholino (LRP6MO, 40 ng) or mRNA (1 ng) cause defects in neural and mesodermal convergent extension. In contrast to uninjected or β-catenin (50 pg) injected siblings, embryos with altered Lrp6 levels are not fully elongated (less than 70% of the length of controls) and have split or thicker notochords resembling that of Xdd- (2 ng) or Dkk1- (400 pg) injected embryos. Lrp6 or β-catenin mRNA levels were chosen so as to cause similar percentages of anterior duplication when injected ventrally (bar graph). For each injection, Tor70 antibody staining for notochord is shown in the lower panels. Scale bars: 0.5 mm. (**B**) The anteriorizing effect of Lrp6MO injection (30 ng) is rescued by co-injecting full-length *lrp6* mRNA (LRP6FL, 500 pg) or β-catenin DNA (100 pg). Convergent-extension defects due to Lrp6MO injections are rescued by co-injecting *lrp6*FL mRNA, but not β-catenin DNA. Anteriorized embryos had an average dorsoanterior index (DAI) of 8 (Kao and Elinson, 1988). β-catenin DNA injection resulted in posteriorized embryos (60% affected, 72 embryos injected) having an average DAI of 2. Error bars indicate standard deviation. Numbers of embryos scored are indicated in parentheses. (**C**) Mesendodermal [Bra (Xbra), Chordin, Goosecoid (Gsc), Sizzled, Endodermin (Endd)] and ectodermal (Otx2, Xag1, epidermal Keratin, Xag1) markers are expressed in developing embryos injected with *lrp6* mRNA (1 ng), *dkk1* mRNA (200 pg) or Lrp6MO (40 ng), indicating that the effect of Lrp6 on convergent extension is not due to altered tissue patterning. Loading control: ODC (ornithine decarboxylase).

For Dsh localization studies, caps were co-injected with 150 pg of *Xenopus* Dsh-GFP and visualized at stage 11 by confocal microscopy (Zeiss Axiovert LSM 510 META; Carl Zeiss, Jena, Germany). Cells with >90% of staining at their cortex were scored as having cortical Dsh-GFP. JNK (also known as Mapk8) activation was assessed in animal caps (stage 11) using phospho-JNK specific antibody (Promega V7931; Promega, Madison, WI, USA). Picture intensity was normalized to control uninjected and β-catenin-injected caps. Cells with exclusive nuclear phospho-JNK staining were counted as positive.

RNA extraction and RT-PCR analysis

Injected animal caps were excised at stage 9, cultured in the presence or absence of activin (10 ng/ml) until stage 11, and RNA was extracted for RT-PCR. Whole embryos were harvested at stage 26. RT-PCR primers and conditions were as previously described (http://www.hhmi.ucla.edu/derobertis/index.html). For each primer set, the appropriate number of cycles within the linear amplification range was determined by testing serial dilutions of reverse-transcribed cDNA. Ornithine decarboxylase mRNA was used as control for RNA extraction and reverse transcription.

TOPFLASH reporter assay

For TOPFLASH reporter assays, HEK293 cells were transiently co-transfected and luciferase activity assessed according to the manufacturer's instructions (Promega, Madison, WI, USA). Assays were performed in triplicate with samples normalized to β-galactosidase.

Open-faced explants, time-lapse imaging, phalloidin staining and Lrp6 localization

Open-faced 'shaved' Keller DMZ and ventral marginal zone (VMZ) explants (Shih and Keller, 1992b) were dissected at stage 10.5 from embryos co-injected with mRNA encoding myristoylated GFP (mGFP) plus *Xenopus* strabismus (*stbm*) mRNA, Lrp6MO, or *lrp6*-B mRNA. Explants were filmed by time-lapse confocal microscopy (Zeiss Axiovert LSM 510 META; Carl Zeiss, Jena, Germany) by capturing one frame every 15 seconds over 15 minutes. Randomly chosen cells from each movie were traced and their motility was measured as described (Tahinci and Symes, 2003). Cell orientations, length-to-width ratios, and protrusion distributions were calculated using ImageJ software (http://rsb.info.nih.gov/ij/) for the middle frame of each movie. Cells from DMZ or VMZ explants were dissociated in 1× modified Barth's saline (MBS) without Ca^{2+} or Mg^{2+} and plated on 200 μg/ml fibronectin (R&D Systems, Minneapolis, MN, USA). After adhering for 30 minutes, cells were fixed and stained with Alexa Fluor 594 phalloidin (Invitrogen, Carlsbad, CA, USA). GFP-positive cells were used for determining morphologies. Length-to-width ratios and protrusion distributions were measured using ImageJ. At least 216 protrusions were measured for each set of injected explants.

For Lrp6 immunolocalization in animal caps, embryos were co-injected with vesicular stomatitis virus G (VSVG)-Lrp6 and mGFP. Embryos were dissected at stage 9 (animal caps) or stage 10.5 (DMZs), fixed at stage 16

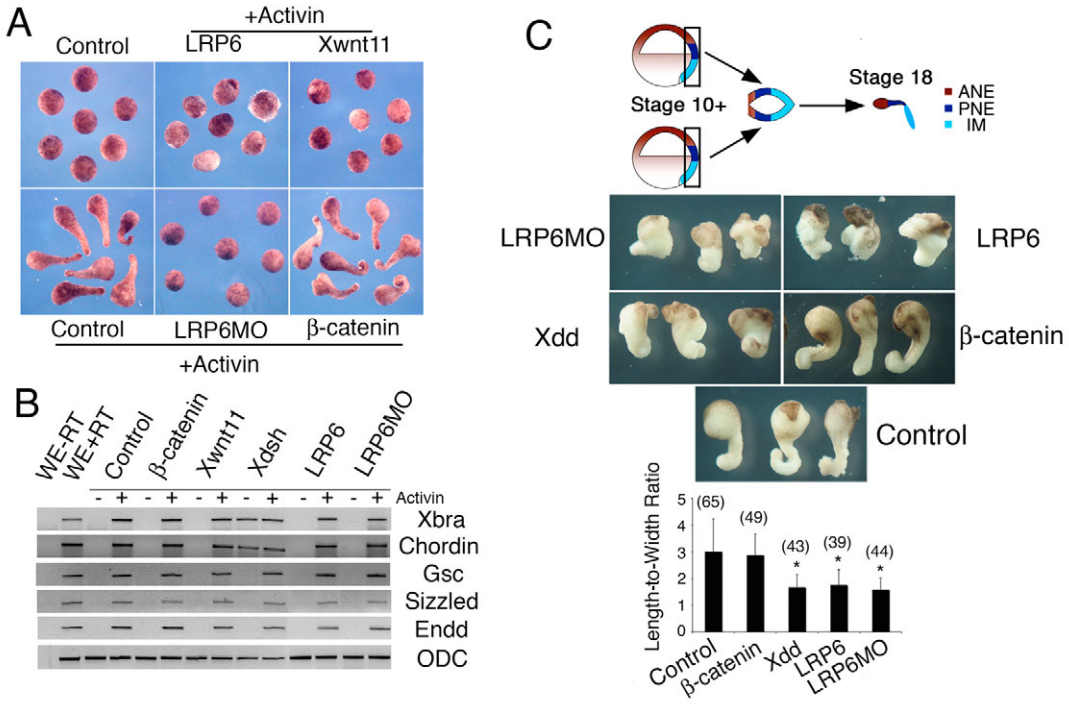

Fig. 2. Loss and gain of Lrp6 function in explants affects convergent-extension movements. (**A**) *lrp6* mRNA (LRP6; 1 ng) or Lrp6MO (LRP6MO; 40 ng) injections block activin-mediated animal cap elongation, in a similar manner to injection of Wnt11 (400 pg) control. By contrast, injection of β-catenin at levels that cause complete axis duplication (50 pg) has no effect. (**B**) RT-PCR analysis shows that mesendodermal markers (Xbra, Chordin, Goosecoid, Sizzled, Endodermin) are induced by activin in animal caps and their expression is unaffected by injections of Lrp6MO or *lrp6* mRNA. Note induction of Xbra and Chordin after injections of similar amounts of *dsh* mRNA (1 ng). Loading control: ODC (ornithine decarboxylase). (**C**) Keller sandwiches elongate when DMZ explants are cultured in apposition. Keller sandwiches injected with Lrp6MO (40 ng) or *lrp6* mRNA (1 ng) show impaired elongation (compared to control uninjected or β-catenin expressing explants) and resemble those expressing Xdd (2 ng). ANE, anterior neural ectoderm; PNE, posterior neural ectoderm; IM, involuting mesoderm. Student's *t*-test was used for statistical analysis. Error bars indicate standard deviation. Asterisks mark differences that are statistically significant from control ($P<0.01$). Numbers of explants scored are indicated in parentheses.

(animal caps) or 11 (DMZs; explants did not undergo appreciable elongation from stage 10.5 to 11), and processed for immunostaining as described previously (Lane and Keller, 1997). For Lrp6 staining in dissociated cells, DMZ explants were dissociated in 1× MBS in the absence of Ca^{2+} or Mg^{2+}, plated on fibronectin-coated slides (200 μg/ml; R&D Systems, Minneapolis, MN, USA), and allowed to adhere for 30 minutes. Cells were fixed in 4% formaldehyde and stained with anti-VSVG-FITC (Bethyl Laboratories, Montgomery, TX, USA) and Alexa Fluor 594 phalloidin (Invitrogen, Carlsbad, CA, USA) as described previously (Sawin et al., 1992).

Antibodies were obtained as follows: rabbit anti-VSVG (Bethyl Laboratories, Montgomery, TX, USA); mouse anti-actin (MP Biomedicals, Solon, OH, USA); Cy2-and Cy3-conjugated secondary antibodies (Jackson Immunoresearch, West Grove, PA, USA). Explants were observed by confocal microscopy (Zeiss Axiovert LSM 510 META; Carl Zeiss, Jena, Germany).

Embryo cryosections

Embryos (stage 10.5) were placed in embedding medium (OCT) with their suprablastoporal regions (prospective chordamesoderm) facing the embedding resin, such that these regions would be sectioned first. Embedded embryos were frozen on dry ice and 10 μm sections were made using a Leica CM3050 S cryostat microtome (Leica Microsystems, Bensheim, Germany). Anti-VSVG (1:200) was applied to sections overnight at 4°C. Sections were incubated with Cy3 secondary antibody (1:200), mounted in antifade (90% glycerol, 4% n-propyl gallate), and examined using the FluoView 100 confocal microscope (Olympus, Tokyo, Japan). Cells with Lrp6 staining extending over less than half of their periphery were scored as having polarized Lrp6 distribution.

RESULTS

Loss or gain of Lrp6 function inhibits convergent extension in *Xenopus* embryos and explants

To assess whether Lrp6 can regulate convergent extension, we performed loss and gain-of-function studies in *Xenopus* embryos. For loss of Lrp6 function, we injected Lrp6 morpholino oligonucleotides (Lrp6MO) to block translation of endogenous *lrp6* mRNA. Lrp6 morphants are anteriorized with expanded heads and cement glands (Fig. 1A), consistent with the established role of Lrp6 in zygotic Wnt/β-catenin signaling. In addition, Lrp6MO-injected embryos fail to fully elongate, consistent with defects in convergent-extension movement during gastrulation. To show specificity for Lrp6 knockdown, we performed rescue experiments. Co-injection of Lrp6MO and full-length *lrp6* mRNA (*lrp6*FL) rescues both elongation and Wnt/β-catenin anteriorization defects (Fig. 1B). By contrast, co-injection of Lrp6MO with β-catenin DNA (which is expressed after the onset of zygotic transcription) suppresses anteriorization, but not embryo elongation defects (Fig. 1B).

For gain of Lrp6 function, we injected mRNA encoding the intracellular domain of Lrp6 fused to an N-terminal myristoylation sequence (Tamai et al., 2004). This construct constitutively transduces the Wnt/β-catenin signal and causes anterior duplication when injected ventrally whereas full-length Lrp6 has only weak

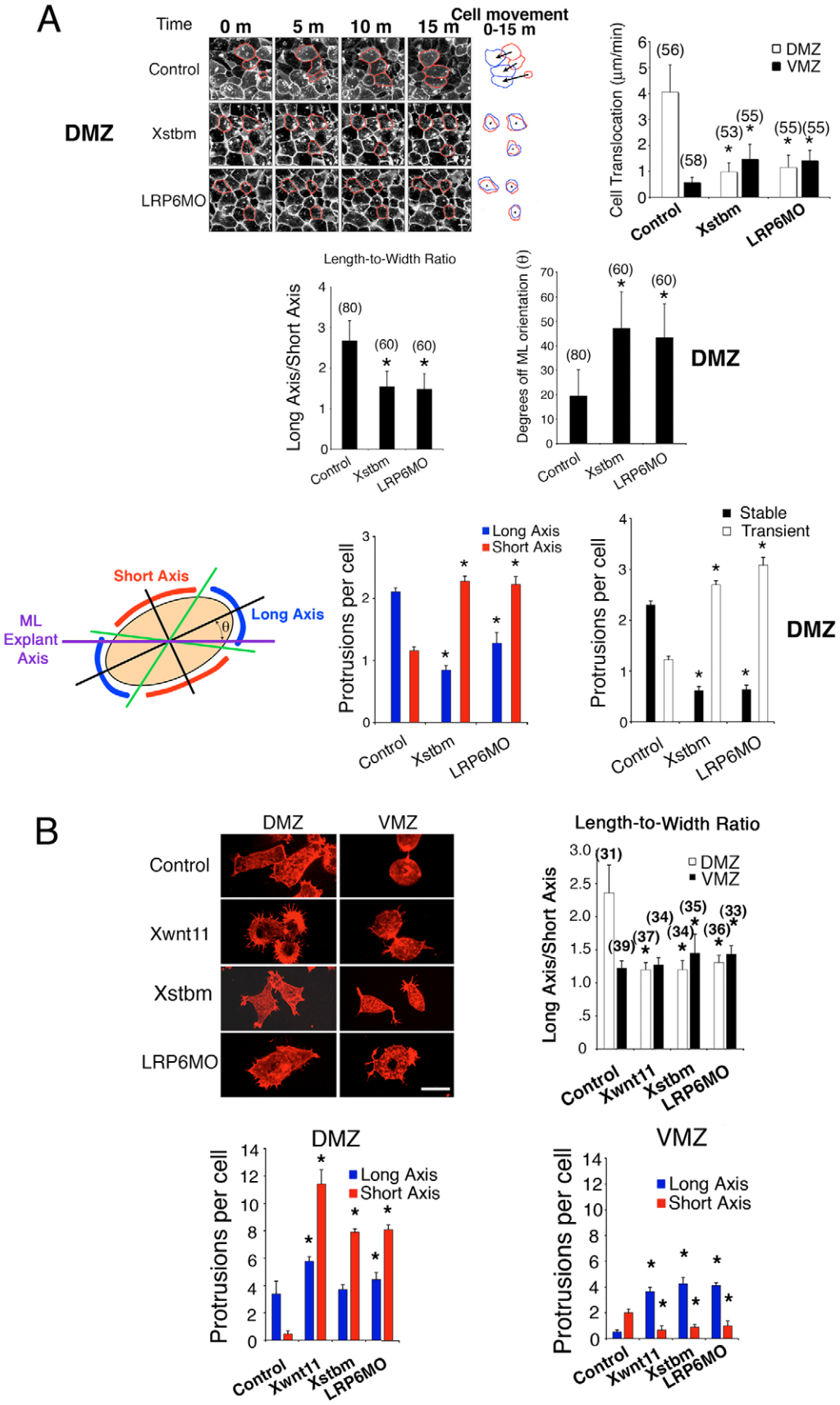

Fig. 3. See next page for legend.

Fig. 3. Lrp6 controls the morphology and motility of mesodermal cells. (**A**) Frames from time-lapse movies of DMZ and VMZ cells in shaved Keller explants from embryos injected with Lrp6MO (LRP6MO; 40 ng) and Stbm (Xstbm; 200 pg) show alterations in motility, shape, orientation, protrusion distribution along the cell periphery and protrusion stability as indicated in the bar charts. Outlines of randomly chosen cells were traced throughout each movie, and traces from the first (red) and last (blue) frame were superimposed to assess cell translocation. For measuring protrusion distributions, each cell was divided into four quadrants emanating from the center (black lines), and each quadrant was subdivided into two sectors by marking the midpoint along the cell membrane (green lines). Each protrusion was assigned to the sector to which it most closely localized (long axis in blue, short axis in red). The angle (θ) between the long axis of the cell and the mediolateral axis (purple line) of the explant was used to calculate its orientation in the explant. Protrusion stability was measured by counting the number of stable (present throughout the 15 minute movie) and transient protrusions (appearing after the first frame and/or disappearing before the last). (**B**) Similar cellular changes were observed in isolated DMZ cells of embryos injected with Lrp6MO. DMZ and VMZ cells from stage 10.5 embryos were dissociated, plated on fibronectin, immediately fixed and stained with Rhodamine-phalloidin. DMZ cells from *wnt11* mRNA (Xwnt; 160 pg)-, *stbm* mRNA (Xstbm; 200 pg)-, or Lrp6MO (LRP6MO; 40 ng)-injected embryos have decreased length-to-width ratios, increased number of total cytoplasmic protrusions, and increased numbers of cytoplasmic protrusions along the short axes versus the long axes compared to GFP-injected (200 pg) control. VMZ cells from *wnt11*-, *stbm*-, or Lrp6MO-injected embryos show no obvious length-to-width ratio changes, but show a greater number of protrusions along their long axes and fewer protrusions along their short axes compared to controls. Statistical analyses in A and B were done using Student's *t*-test. Error bars indicate standard deviation. Asterisks mark differences that are statistically significant from control ($P<0.01$). Numbers of cells analyzed are indicated in parentheses. DMZ and VMZ cells used to determine length-to-width ratios were also used to determine number of protrusions per cell. Cells and explants were co-injected with myristoylated GFP (200 pg) to highlight plasma membranes and trace injected cells. Scale bars: 25 μm in A; 20 μm in B.

canonical activity (Fig. 1A). Unless otherwise indicated, this constitutively active construct was used in all subsequent studies. Embryos injected in their presumptive neural ectoderm (dorso-animal blastomeres) fail to fully elongate their anteroposterior (AP) axes and develop with dorsal flexure; they have bifurcated, bent notochords, suggestive of defects in neural convergent extension (Wallingford and Harland, 2001). Embryos injected in their presumptive axial mesoderm (dorsovegetal blastomeres) develop with closed neural tubes, but have shortened AP axes with thicker notochords, suggestive of defective mesodermal convergent extension (Fig. 1A). Similar phenotypes are observed when embryos are injected with Xdd, a dominant negative mutant of Dishevelled that affects convergent extension (Sokol, 1996). The ability of Lrp6 to block gastrulation or neurulation cannot be attributed to Wnt/β-catenin pathway activation because functionally equivalent amounts of β-catenin mRNA that cause a similar percentage of anterior duplication (injected ventrally) do not block AP axis elongation when injected into dorsal blastomeres (Fig. 1A). These results are reminiscent of studies of Wnt/PCP components in that either loss or gain of Lrp6 function causes gastrulation and/or neurulation defects (Ueno and Greene, 2003), depending on the injection site.

The gastrulation defects observed in embryos with loss or gain of Lrp6 function can be attributed to either defective patterning or morphogenesis of developing tissues. To distinguish between these two possibilities, we performed RT-PCR analysis of tissue-specific marker genes. We detect proper mesendoderm specification in embryos injected with either Lrp6MO or *lrp6* mRNA as evidenced by expression of the following markers: Brachyury (pan-mesodermal); Goosecoid and Chordin (anterior mesodermal); Sizzled (posterior mesodermal); and the endodermal marker Endodermin (Fig. 1C). Anterior neural tissue is also present in these embryos as evidenced by expression of Otx2 and Xag1. Lrp6 downregulation by morpholino injection causes a concomitant decrease in expression of epidermal keratin, consistent with anteriorization of neural ectoderm at the expense of epidermis in the absence of Wnt/β-catenin signaling (Glinka et al., 1998). These results show that either gain or loss of Lrp6 causes defects in morphogenesis rather than mesendodermal tissue patterning.

We next assessed the role of Lrp6 in regulating convergent extension using *Xenopus* explants, animal caps and Keller sandwiches (Symes and Smith, 1987; Keller and Danilchik, 1988). Animal caps from *Xenopus* blastulae differentiate into round epidermal tissue when cultured in vitro. In the presence of mesoderm-inducing activin, however, their cells intercalate, resulting in cap elongation (Symes and Smith, 1987). Injection of activators or inhibitors of Wnt/PCP signaling blocks this elongation process (Simons et al., 2005; Takeuchi et al., 2003). Animal caps from embryos injected with *lrp6* mRNA or Lrp6MO fail to elongate with activin treatment, resembling caps injected with Wnt11, an activator of Wnt/PCP signaling (Fig. 2A). Inhibition of elongation in *lrp6* mRNA- and Lrp6MO-injected caps occurs despite proper induction of mesendodermal markers, confirming that loss and gain of Lrp6 function result in inhibition of convergent extension (Fig. 2B). Furthermore, this inhibition induced by Lrp6 loss of function cannot be rescued by co-injection of β-catenin mRNA, confirming that Lrp6 blocks convergent-extension movements in a β-catenin-independent manner (see Fig. S1 in the supplementary material).

Keller sandwiches consist of two apposed dorsal marginal zone (DMZ) explants that elongate as a result of convergent extension of their neural and mesodermal tissues (Keller and Danilchik, 1988). Keller sandwiches were formed from embryos injected with either Lrp6MO or *lrp6* mRNA, and their elongation was assessed at stage 18. These explants were unable to fully elongate compared with control explants (Fig. 2C), which indicates defective convergent extension. Again, the effect of Lrp6MO in blocking explant elongation was not rescued by co-injection of β-catenin mRNA (see Fig. S1 in the supplementary material). Taken together, our embryo and explant data support a role for Lrp6 in controlling convergent-extension movements during early *Xenopus* embryogenesis.

Lrp6 affects mesodermal cell morphology, motility and actin rearrangement

Cell intercalation drives mesodermal convergent extension during vertebrate development. To intercalate, cells acquire an elongated shape and form cytoplasmic processes along their long axes. These changes in morphology are thought to be actin driven (Keller et al., 2003).

To assess whether the overall morphology, arrangement and motility of marginal zone cells is affected by loss of Lrp6 function, we performed live cell analysis in open-faced 'shaved' Keller explants (Shih and Keller, 1992a) from the marginal zone (Tahinci and Symes, 2003). Stbm, a Wnt/PCP signaling component, has been shown to block convergent extension in

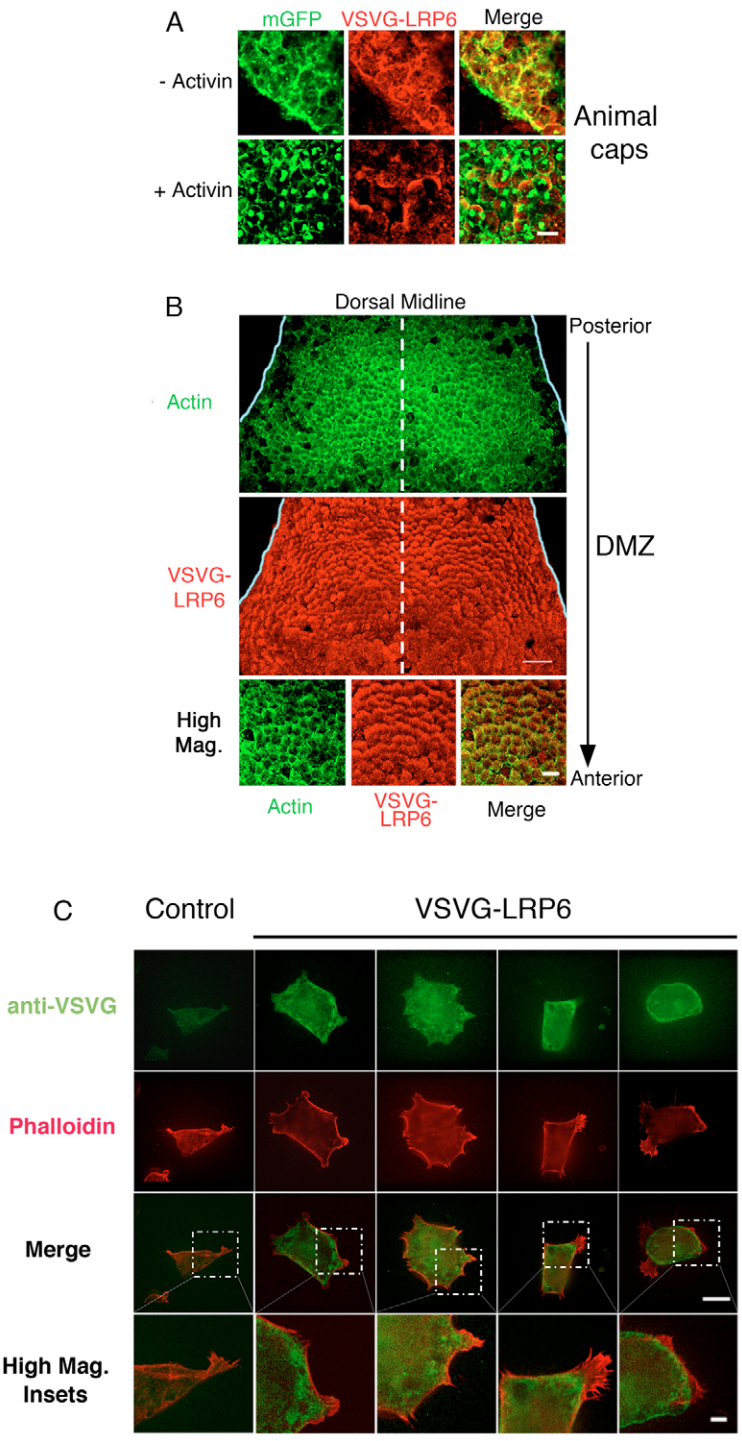

Fig. 4. Lrp6 localizes in a polarized distribution in cells that undergo convergent extension and is adjacent to actin-rich regions in cellular processes. (**A**) Animal cap cells show uniform distribution of injected VSVG-*lrp6* (VSVG-LRP6; 2 ng). In Activin-treated caps the staining of VSVG-Lrp6 is polarized. (**B**) DMZ explants from VSVG-Lrp6-injected embryos show preferential localization of Lrp6 at the posterior cell edge. High magnification views of cells in the DMZ are shown in the bottom panels. Injection of myristoylated, plasma membrane localized GFP (mGFP; 500 pg) or anti-actin staining was performed as controls for animal cap and DMZ experiments, respectively. Explants are outlined with solid lines to make their borders readily identifiable. (**C**) Lrp6 is adjacent to actin-rich regions of cellular extensions. DMZ cells injected with VSVG-Lrp6 were dissociated, plated on fibronectin, immediately fixed, and stained with anti-VSVG (green) and phalloidin (red). Scale bars: animal caps, 30 μm; DMZ (40×), 200 μm; high-magnification DMZ (75×), 50 μm; dissociated cells (200×), 20 μm; high-magnification dissociated cells (350×), 5 μm.

dorsal explants (Darken et al., 2002). Shaved Keller explants of DMZ cells injected with Lrp6MO show slower motility and resemble cells overexpressing Stbm (Fig. 3A). Cells in these explants have smaller length-to-width ratios (i.e. rounder) and reduced ability to orient along the mediolateral embryonic axis compared to control. Protrusions of these cells are predominantly oriented along their short axes and are transient compared with those of control cells, resembling cells overexpressing Stbm. Ventral marginal zone (VMZ) cells injected with stbm mRNA or Lrp6MO show increased cell motility, reflecting possible stimulation of Wnt/PCP signaling (Fig. 3A).

To determine whether Lrp6 downregulation can also promote changes in the behavior of isolated cells, we assessed the morphology of cells dissociated from the DMZ or VMZ of Lrp6MO-injected embryos (Fig. 3B). The majority of DMZ cells from GFP-injected control embryos become elongated with cytoplasmic protrusions along their long axes. Equivalently staged VMZ cells, by contrast, are round with most protrusions distributed along their short axes. DMZ cells from Lrp6MO-injected embryos are rounder than controls and have a large number of protrusions around their periphery; a similar phenotype is observed for DMZ cells injected with Wnt11 or Stbm, regulators of Wnt/PCP signaling.

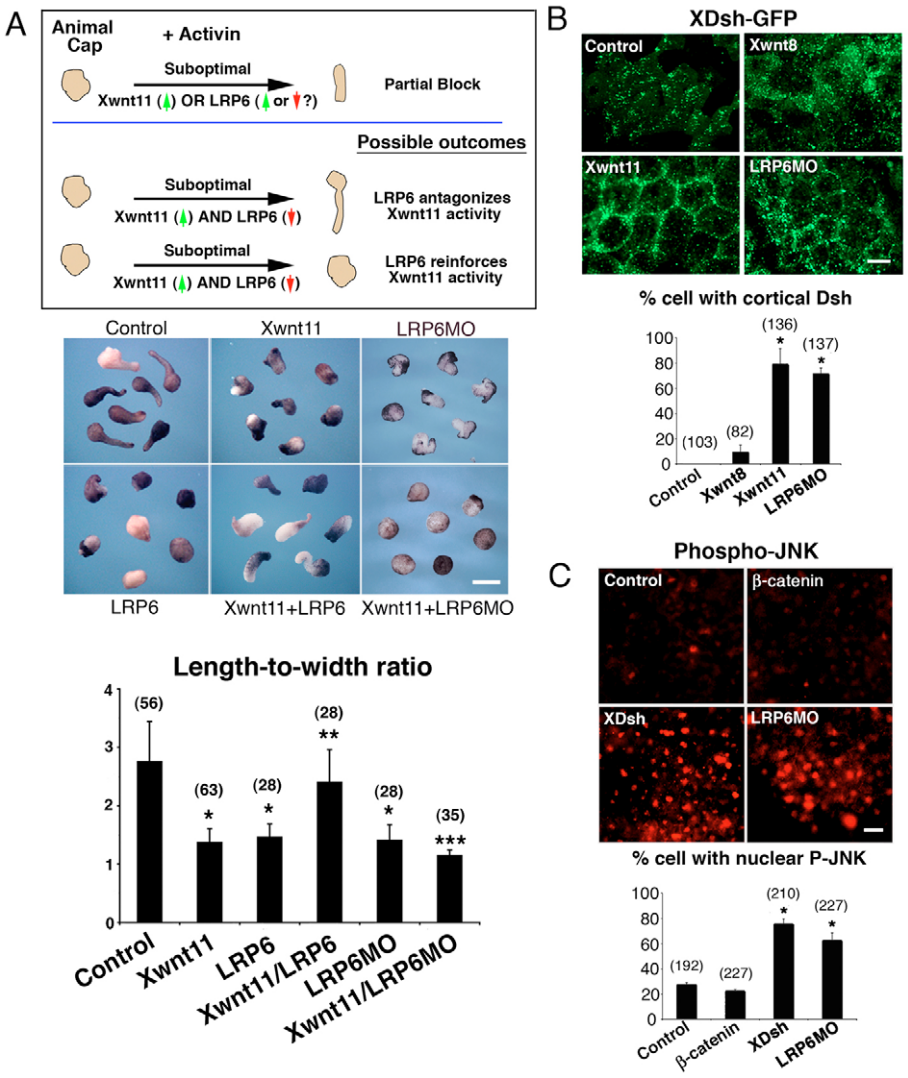

Fig. 5. Lrp6 antagonizes Wnt/PCP signaling upstream of Dishevelled and JNK. (**A**) Injection of suboptimal amounts of *wnt11* mRNA (Xwnt; 160 pg), an activator of Wnt/PCP signaling, or suboptimal amounts of *lrp6* mRNA (LRP6; 1 ng) causes incomplete block of activin-induced animal cap elongation. Injection of suboptimal *lrp6* mRNA (1 ng) reverses the partial block by Wnt11 (160 pg) of activin-mediated animal cap elongation, suggesting that Lrp6 opposes Wnt11-mediated activation of the Wnt/PCP pathway. Injection of suboptimal Lrp6MO (30 ng) reinforces the Wnt11-mediated partial block of activin-treated animal caps, further demonstrating that Lrp6 antagonizes Wnt/PCP signaling. Double asterisks for Wnt11+Lrp6 (Xwnt11/LRP6) indicate statistically significant differences from Wnt11 and Lrp6 (P<0.01). Triple asterisks for Wnt11+Lrp6MO mark differences statistically significant from Wnt11 and Lrp6MO (P<0.01). (**B**) Dsh-GFP translocates to the cell cortex upon Wnt/PCP activation. Injection of Wnt11 (400 pg) or Lrp6MO (40 ng) promotes cortical translocation of Dsh-GFP. By contrast, injection of the Wnt/β-catenin ligand, Wnt8 (Xwnt; 40 pg), has no significant (bar chart) effect on XDsh-GFP localization. (**C**) Jun-N-terminal kinase (JNK) is phosphorylated and localized to the nucleus in animal caps injected with dsh (XDsh; 1 ng) (160 pg) or Lrp6MO (40 ng). Animal caps injected with β-catenin mRNA (50 pg) demonstrate minimal phospho-JNK staining or nuclear localization similar to uninjected control. Student's t-test was used for statistical analysis. Error bars indicate standard deviation. Asterisks mark differences that are statistically significant from control (P<0.01). Numbers of explants/cells scored are indicated in parentheses. Scale bars: 500 μm in A; 50 μm in B; 100 μm in C.

VMZ cells injected with Wnt11 or Stbm are rounder than control cells and have a greater number of small processes along their long axes; VMZ cells injected with Lrp6MO are slightly more elongated than control cells and similarly have a large number of protrusions along their long axes. Together, the effects of loss of Lrp6 function on the morphology of cells from marginal zone tissues resemble those of Wnt11 and Stbm. We propose that these differences in the morphologies of cells isolated from control versus Lrp6 morphant embryos may also affect the behavior of these cells in the context of an embryo or explant.

Lrp6 is localized in a polarized fashion in dorsal marginal zone cells

In the *Drosophila* wing, proteins that confer planar cell polarity through Wnt/PCP signaling are asymmetrically distributed in epithelial cells: inhibitors localize proximally and activators distally (Klein and Mlodzik, 2005). In vertebrates, asymmetric distribution of several Wnt/PCP components has also been reported: Dvl2 (Wang et al., 2005), prickle (Ciruna et al., 2006) and PKC (Kinoshita et al., 2003).

We tested whether Lrp6 has a polarized distribution in intercalating mesodermal cells. Animal caps injected with VSVG-*lrp6* mRNA show a uniform subcellular staining pattern (Fig. 4A). Strikingly, treatment of animal caps with activin at concentrations that induce dorsal mesoderm and promote elongation (via a mechanism that is believed to recapitulate convergent extension) causes, indirectly, asymmetric relocalization of Lrp6 (Fig. 4A). Confirming these findings, cryosections of whole embryos injected with VSVG-*lrp6* show that Lrp6 has a uniform distribution in cells of the animal pole and VMZ in early gastrulae, but not the DMZ (see Fig. S2 in the supplementary material). This spatial distribution of Lrp6 is reminiscent of the localization of inhibitory PCP proteins in the *Drosophila* wing and eye (Klein and Mlodzik, 2005).

We also observe a polarized subcellular distribution for Lrp6 in whole DMZ explants. Embryos were injected with VSVG-tagged *lrp6* mRNA (at a concentration that did not perturb embryonic morphology), and open-faced shaved Keller explants of the DMZ were stained with anti-VSVG antibody. To more faithfully assess Lrp6 localization, explants were not cultured prior to fixation and staining for Lrp6. VSVG-Lrp6 predominantly localized to the posterior surface of intercalating DMZ cells throughout the whole explant (Fig. 4B). This distribution of VSVG-Lrp6 in DMZ cells is unlikely to be due to oriented anteroposterior cell overlapping (Winklbauer and Nagel, 1991) because cortical actin staining can clearly be seen at anterior and posterior surfaces of these cells.

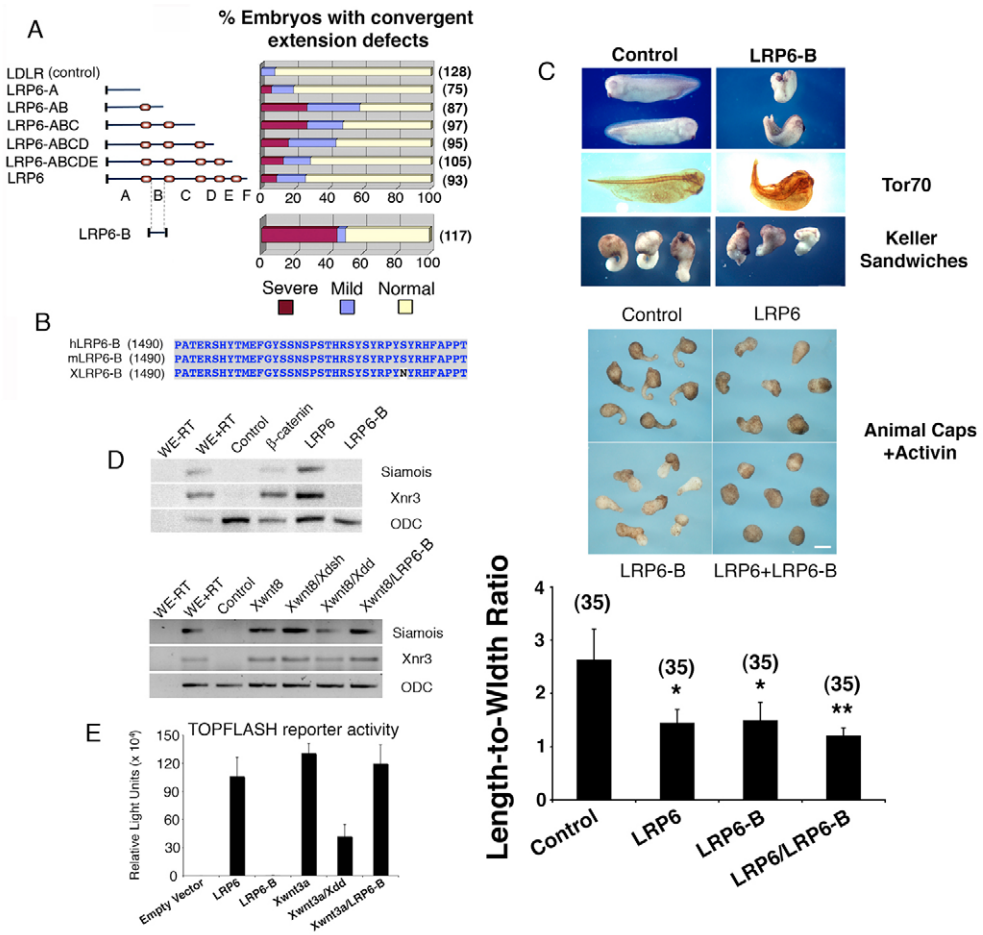

Fig. 6. A small intracellular domain of Lrp6 is sufficient to mediate its convergent-extension activity. (**A**) Serial deletions of the intracellular domain of Lrp6 demonstrate that a 36 amino acid fragment, Lrp6-B, can mediate its convergent-extension activity. Dark red boxes indicate PPP(S/T)P motifs. All constructs have an N-terminal myristoylation sequence. Percentages of normal (>70% ACEL; average control embryo length), mildly affected (30-70% ACEL), or severely affected (<30% ACEL) embryos are shown (bar graph). Each construct (500 pg mRNA) was used in at least three independent experiments. Numbers of embryos scored are shown in parentheses. (**B**) Sequence comparison of the B domain of human Lrp6 (hLRP6-B), mouse Lrp6 (mLRP6-B) and *Xenopus* Lrp6 (XLRP6-B). Numbers in parentheses indicate the amino acid position of the start of the B domain. Identical amino acids are in blue. (**C**) Embryos and explants from embryos injected with *lrp6*-B mRNA (2 ng) show severe convergent-extension defects; Lrp6-B (1.6 ng) synergizes with Lrp6 (1 ng) in blocking animal cap elongation. Lateral views of stage 26 embryos are shown. In the bar graph, single asterisks indicate statistically significant differences from control ($P<0.01$), and double asterisks indicate statistically significant differences from Lrp6 and Lrp6-B values ($P<0.01$). Numbers of caps scored are indicated in parentheses. (**D**) Lrp6-B does not induce expression of Wnt/β-catenin target genes, siamois and *nr3* (Xnr3), or act in a dominant-negative manner to inhibit Wnt8-induced expression of siamois and *nr3* in animal caps. Loading control: ODC (ornithine decarboxylase). Whole embryos (WE) were used as positive control. RT, reverse transcriptase. (**E**) In contrast to dominant negative Dishevelled (Xdd), transient transfection of Lrp6-B in HEK293 cells does not upregulate TOPFLASH or inhibit Wnt3a-induced TOPFLASH activity. Student's *t*-test was used for statistical analysis. Error bars indicate standard deviation. Scale bar: 500 μm in C.

Reorganization of the actin cytoskeleton is a major consequence of Wnt/PCP signaling. The mechanism by which Wnt/PCP signaling impinges on the cytoskeleton, however, is still poorly understood, and a direct link between Wnt/PCP components and the actin cytoskeleton has not been established. Thus, we sought to establish an association between the actin cytoskeleton and Lrp6, a potential regulator of Wnt/PCP signaling. We injected cells of the DMZ with VSVG-*lrp6* mRNA, dissociated cells at stage 10.5, and stained them with anti-VSVG antibody and Rhodamine-phalloidin (Fig. 4C). Lrp6 was seen at the periphery of cells and was enriched adjacent to actin-rich cortical areas of cellular protrusions. This observation suggests a potential role for Lrp6 in regulating the actin cytoskeleton and is consistent with our proposed role for Lrp6 in polarized cell movement and regulation of convergent extension.

Lrp6 negatively regulates Wnt/PCP signaling

Injection of either positive or negative regulators of Wnt/PCP signaling into animal caps inhibits explant elongation, thereby demonstrating the importance of spatial and temporal organization for proper signaling (Penzo-Mendez et al., 2003; Takeuchi et al., 2003). To determine whether Lrp6 is a positive or negative Wnt/PCP regulator, we tested the ability of Lrp6 to oppose or reinforce the effect of sub-optimal amounts of co-injected Wnt11 by tipping the balance towards increased Wnt11 signaling (i.e. Lrp6 strengthens the Wnt11 effect) or decreased Wnt11 signaling (i.e. Lrp6 weakens the Wnt11 effect; Fig. 5A). Injection of sub-optimal amounts of Lrp6 opposes Wnt11-induced inhibition of animal cap elongation, indicating that Lrp6 is a negative regulator of Wnt/PCP signaling. Similarly, sub-optimal amounts of Wnt11 are reinforced by Lrp6MO in

potentiating inhibition of animal cap elongation, further indicating that Lrp6 downregulates Wnt/PCP signaling (Fig. 5A).

To further address the role of Lrp6 as a negative regulator of Wnt/PCP signaling, we assayed downstream molecular events. In unstimulated cells and cells with active Wnt/β-catenin signaling, injected Dsh-GFP is predominantly cytoplasmic with a punctate pattern (Yanagawa et al., 1995). Upon activation of Wnt/PCP signaling, Dsh-GFP localizes predominantly to the cell cortex (Yanagawa et al., 1995). Cortical localization of Dsh-GFP is readily observed in animal caps expressing Wnt11 (Fig. 5B). Consistent with activation of the Wnt/PCP pathway, Lrp6MO injection also results in Dsh-GFP localization to the cortex. As a control, injection of animal caps with Wnt8, which signals through the Wnt/β-catenin pathway, does not cause cortical redistribution of Dsh-GFP.

JNK is phosphorylated as a result of Wnt/PCP signaling (Yamanaka et al., 2002). Animal caps expressing Dsh or Lrp6MO show enhanced nuclear phospho-JNK staining consistent with their roles as Wnt/PCP activators (Fig. 5C). By contrast, β-catenin injections do not affect phospho-JNK. These results provide molecular evidence that Lrp6 antagonizes Wnt/PCP signaling.

A 36-residue intracellular domain of Lrp6 is sufficient to mediate its effects on convergent extension

To determine the region of Lrp6 responsible for mediating its Wnt/PCP activity, we performed structure-function analysis of its intracellular domain. Previous studies have shown that the intracellular domain of Lrp6 contains five PPP(S/T)P motifs, each of which can activate Wnt/β-catenin signaling (Tamai et al., 2004). C-terminal deletion mutants of Lrp6 lacking these motifs were tested for their ability to perturb convergent extension in embryos (Fig. 6A).

Embryos injected with various Lrp6 constructs were scored as normal, or affected (mildly or severely) based on AP axes lengths as previously described (Goto and Keller, 2002). Surprisingly, progressive C-terminal deletions of Lrp6 result in an increasing percentage of elongation defects until a 36-residue fragment (Lrp6-B) is eliminated (Fig. 6A,B). Similar to injections of Lrp6, injections of Lrp6-B result in severe mesodermal and neural convergent-extension defects in embryos, animal caps and Keller sandwiches (Fig. 6C). In addition, Lrp6-B potentiates the effect of Lrp6 in blocking animal cap elongation, indicating that Lrp6-B regulates convergent-extension activity in the same direction as the full-length intracellular domain (Fig. 6C). Finally, Lrp6-B reverses the Lrp6MO-mediated block in elongation of animal caps (see Fig. S3A in the supplementary material) and Keller sandwich explants (see Fig. S3B in the supplementary material), indicating that it is sufficient to transduce a signal to the PCP branch of the Wnt pathway. RT-PCR analysis of animal caps and TOPFLASH reporter assays in HEK-293 cells reveal that Lrp6-B is unable to activate β-catenin-dependent transcription (Fig. 6D,E) or to act in a dominant-negative manner to inhibit Wnt-mediated induction of β-catenin targets (Fig. 6D,E). Thus, Lrp6 appears to mediate its convergent-extension activity through Lrp6-B, independent of its role in regulating β-catenin-mediated transcription (Yokota et al., 2003). This result is consistent with our observation that co-injection of β-catenin rescues the defects in Wnt/β-catenin, but not Wnt/PCP signaling caused by injection of Lrp6MOs into *Xenopus* embryos and explants (Fig. 1B and see Fig. S1A,B in the supplementary material).

Phalloidin staining of DMZ and VMZ cells expressing Lrp6-B reveals that this domain of Lrp6 alters the bipolar morphology of cells in the DMZ (see Fig. S2C in the supplementary material) without activating cell motility in the VMZ (see Fig. S2D in the supplementary material) or Wnt/PCP downstream events (e.g. Dsh localization or JNK phosphorylation; see Fig. S2E in the supplementary material). Injection of *lrp6-B* mRNA causes dramatic changes in the protrusive activity of DMZ and VMZ cells (see Fig. S2C in the supplementary material). Similar results were obtained by injection of the entire intracellular domain of Lrp6 (data not shown), further indicating that Lrp6-B can recapitulate the effects of Lrp6 on convergent extension.

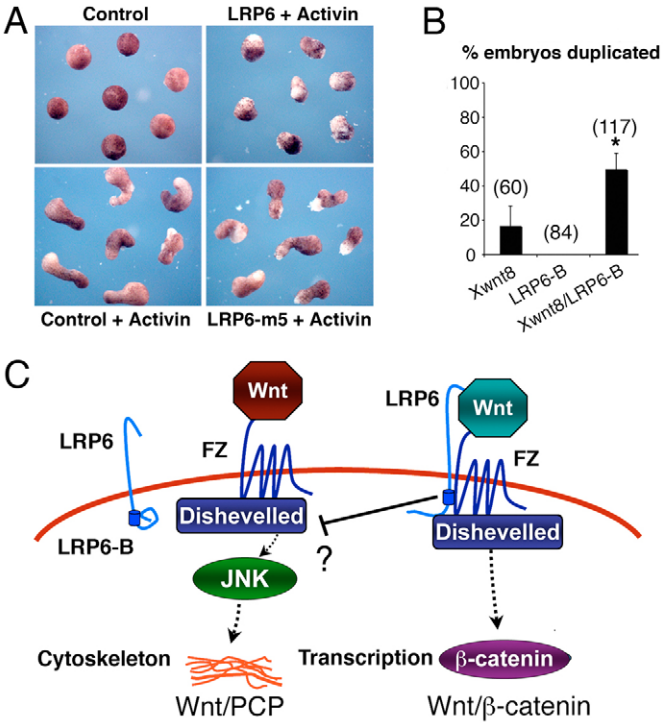

Fig. 7. Evidence for coupling of Lrp6 functions: inhibition of Wnt/PCP signaling and activation of Wnt/β-catenin signaling. (**A**) In contrast to Lrp6, injection of a mutant Lrp6 that cannot activate the Wnt/β-catenin pathway (LRP6-m5) does not inhibit activin-mediated elongation of animal caps. Equivalent amounts of *lrp6* or *lrp6*-m5 mRNA (2 ng) were injected. (**B**) *lrp6*-B mRNA (3 ng) alone does not induce secondary axis formation in *Xenopus* embryos, but potentiates the activity of *wnt8* mRNA (6 pg) in secondary axis assays. Numbers of embryos injected are shown in parentheses. Asterisk indicates statistically significant differences ($P<0.01$). (**C**) Model in which Wnt ligands promote assembly of active Lrp6/Frizzled (FZ) receptor complexes that recruit Dishevelled and actively inhibit Wnt/PCP signaling (via as yet unknown mechanisms) through the B domain of Lrp6.

Coupling of the Wnt/β-catenin and Wnt/PCP pathways at the level of Lrp6

Identification of Lrp6-B as a region of Lrp6 that can inhibit Wnt/PCP signaling without activating Wnt/β-catenin targets indicates that these two activities of Lrp6 require distinct domains. It is not clear, however, whether they are physiologically coupled. To address this question, we used a non-phosphorylatable mutant of the intracellular domain of Lrp6, Lrp6-m5, in which all serine/threonine residues within the PPP(S/T)P motifs are replaced by alanines. This mutant, which contains the Lrp6-B sequence, acts in a dominant-negative manner to inhibit Wnt/β-catenin signaling (Tamai et al., 2004). Interestingly, injection of Lrp6-m5 at concentrations that block Wnt/β-catenin signaling by RT-PCR (data not shown) failed to inhibit animal cap elongation (Fig. 7A), suggesting that Lrp6 phosphorylation is

necessary for Lrp6 to mediate its Wnt/PCP activity (possibly by relieving steric inhibition to expose the Lrp6-B region). This result is consistent with our observation of increased Wnt/PCP activity upon progressive C-terminal truncations of Lrp6 regions necessary for Wnt/β-catenin signaling (Fig. 6A).

Activation of Wnt/PCP signaling has been suggested to antagonize Wnt/β-catenin signaling (Peters et al., 1999; Yan et al., 2001; Kuhl et al., 2001; Schwarz-Romond et al., 2002). To test whether inhibition of this antagonistic activity is sufficient to promote Wnt/β-catenin signaling, we co-injected Lrp6-B mRNA with sub-optimal amounts of the Wnt/β-catenin ligand, Wnt8, and scored embryos for axis duplication, an in vivo read-out for Wnt/β-catenin activation. Lrp6-B injection potentiates the effects of Wnt8 in inducing axis duplication (Fig. 7B), indicating that inhibition of Wnt/PCP signaling at the level of Lrp6 potentiates Wnt/β-catenin signaling. Based on these findings, we propose a model in which Lrp6, through its interactions with cytoplasmic factors via an intracellular 36-residue domain, acts as a switch between Wnt/β-catenin and Wnt/PCP signaling (Fig. 7C).

DISCUSSION

In our current study, we show that Lrp6 regulates convergent-extension movements by downregulating Wnt/PCP signaling. Using gain- and loss-of-function studies in *Xenopus* embryos and explants, we show that Lrp6 regulates convergent-extension movements without affecting mesodermal tissue patterning. Lrp6 controls the shape, polarity and motility of mesodermal cells and is asymmetrically localized to the posterior surface of cells that undergo convergent extension. We show that Lrp6 antagonizes the activity of Wnt11, an activator of Wnt/PCP signaling, in an animal cap elongation assay and that Lrp6MO potentiates the activity of Wnt11 in this assay. Furthermore, we detect enhanced cortical localization of Dsh and phosphorylation of JNK in Lrp6 morphant tissues, both of which are consistent with a role for Lrp6 as an inhibitor of Wnt/PCP signaling. We have identified a 36-residue domain of Lrp6 with Wnt/PCP activity that is distinct from the previously characterized PPP(S/T)P motifs of Lrp6 that are necessary for Wnt/β-catenin signaling. Based on these findings, we propose a model in which Lrp6 regulates convergent extension by coordinating a molecular switch from Wnt/PCP to Wnt/β-catenin signaling.

The role of Lrp6 in mediating the switch from Wnt/PCP to Wnt/β-catenin signaling

From this study we provide evidence for interaction between the Wnt/β-catenin and Wnt/PCP pathways at the level of Lrp6. We show that injection of mRNA encoding a small intracellular domain of Lrp6, Lrp6-B, inhibits Wnt/PCP signaling while potentiating Wnt/β-catenin signaling. Our data also indicate that Lrp6 activation (via activation of Wnt/β-catenin signaling) is a prerequisite for its ability to inhibit Wnt/PCP signaling (Fig. 7C). Our data suggest that coupling of Wnt/PCP inhibition with activation of Wnt/β-catenin is embedded at the structural level of Lrp6.

Because Lrp6 activation is necessary for inhibition of Wnt/PCP, it stands to reason that canonical Wnt inhibitors that bind Lrp6 (e.g. Dkks, SOST) would potentiate the Wnt/PCP pathway by relieving inhibition by Lrp6. Wnt-Fz-Lrp6 interactions can in turn be influenced by tissue-specific factors, depending on the context (Tao et al., 2005). This model is reminiscent of the Hedgehog signaling pathway where signaling occurs through another seven-pass transmembrane protein, Smoothened, upon relief of inhibition by the Hedgehog receptor, Patched (Cohen, 2003).

Inhibition of Wnt/PCP by Lrp6 occurs through intracellular interactions

Recently, Dkk1 has been proposed to activate Wnt/PCP signaling by interacting with glypican 4 (Caneparo et al., 2007). Our observation that Lrp6 inhibits Wnt/PCP signaling is unlikely to be a consequence of disruption of the Dkk1-glypican 4-mediated activation of Wnt/PCP signaling because our gain-of-function studies were conducted with the intracellular domain of Lrp6, which presumably cannot bind to Dkk1, a secreted protein. Based on our results, it is possible that some of the effect of Dkk1 on Wnt/PCP signaling may be indirectly due to its interaction with Lrp6. Interestingly, Wise, a context-dependent activator or inhibitor of Wnt signaling, can both bind Lrp6 and affect Wnt/PCP signaling, as evidenced by its ability to block elongation in activin-treated animal caps (Itasaki et al., 2003).

One obvious mechanism by which Lrp6 could inhibit Wnt/PCP signaling would be through its interaction with the scaffold protein Axin. Axin can bind directly to Dsh (Li et al., 1999), and it is possible that, indirectly, Lrp6 could decrease the activity of Dsh in the Wnt/PCP pathway and concomitantly increase its activity in the Wnt/β-catenin pathway. We believe that this scenario is unlikely because the Lrp6 regions that have been shown to bind Axin and mediate Wnt/β-catenin signaling, the PPP(S/T)P motifs, are distinct from the Lrp6 domain that we show inhibits Wnt/PCP signaling. It is possible that Lrp6 directly interacts with Dsh to inhibit Wnt/PCP signaling. To our knowledge, however, there has been no reported interaction between Lrp6 and Dsh, and we have been unsuccessful in demonstrating interaction between either the full intracellular domain of Lrp6 or Lrp6-B and Dsh (data not shown). Thus, we favor a model in which Lrp6 mediates its Wnt/PCP activity through its interaction with Wnt/PCP pathway components that function downstream of Dsh.

Lrp6 localizes to the posterior edge of intercalating axial mesodermal cells

Core Fz/PCP components have been shown to have asymmetrical subcellular localization patterns in *Drosophila* wing cells. Positive regulators of Fz/PCP signaling are localized distally at the site of actin-rich hair formation, whereas negative regulators are localized proximally (reviewed by Jenny and Mlodzik, 2006). Similar observations have been made in cochlea sensory hair cells of vertebrates. For example, Dvl2 is localized to the site of actin-rich stereocilia formation (Wang et al., 2005) in the outer cell cortex, whereas Vangl2 [the mouse ortholog of Stbm; Montcouquiol et al. (Montcouquiol et al., 2006)] is localized to the opposing inner side.

Demonstration of asymmetric subcellular localization of Wnt/PCP components during vertebrate convergent extension has been less straightforward. Initial studies in cultured *Xenopus* explants indicated that Dsh and PKC are enriched along the mediolateral axis of cells undergoing convergent extension (Kinoshita et al., 2003). Prickle, a Wnt/PCP regulator that interacts with Dsh, has recently been shown to localize to the anterior end of notochord and neurectoderm cells during zebrafish neurulation (Ciruna et al., 2006). We have, however, been unable to observe polarized localization of either Dsh-GFP or GFP-Prickle in the DMZ. Furthermore, their localization is not altered by injection of *lrp6* mRNA or Lrp6MO (data not shown).

Our results show that Lrp6, a core component of the Wnt/β-catenin pathway, is localized to the posterior end of intercalating mesodermal cells of the early *Xenopus* gastrula. It is tempting to speculate that Lrp6 may indirectly inhibit Dsh activity in the posterior end of these cells during gastrulation. Interestingly, these mesodermal cells intercalate in a mediolateral fashion, perpendicular to the axis of Lrp6 polarization. This suggests that other signaling pathways (in addition

to Wnt/PCP) may also act to control cell polarity during convergent extension (Hyodo-Miura et al., 2006). Further characterization of the Wnt/PCP signaling cascade downstream of Lrp6 will probably provide clues as to the spatial and temporal activation of Wnt/PCP components during vertebrate convergent extension.

We thank Richard Harland, Randy Moon, Eddie de Robertis, Xi He, Keiko Tamai and Kristen Kwan for generous gifts of reagents. We are also grateful to Liliana Solnica-Krezel, Chris Wright, David Greenstein and Karen Symes for critically reviewing the manuscript and providing valuable comments. We also thank Michael Anderson, Chris Cselenyi, Kristin Jernigan, Yuki Ohi, J.J. Westmoreland, Andrey Efimov, Priscilla Fonseca-Siesser and Leslie Meenderink for technical advice. Erin Loggins, Jun Dou and Joshua Tarkoff provided excellent technical assistance. These studies were funded by an American Cancer Society Research Scholar Grant (RSG-05-126-01 to E.L.), a Biomedical Scholarship from the Pew Charitable Trusts, a Molecular Endocrinology (NIH) Training Grant (5 T 32 DK007563 to C.A.T.), and an America Heart Association predoctoral fellowship (0615279B to C.A.T.). R.J.C. was funded by grants CA46413, GI SPORE P50 95103, and MMHCC U01 084239.

Supplementary material

Supplementary material for this article is available at
http://dev.biologists.org/cgi/content/full/134/22/4095/DC1

References

Caneparo, L., Huang, Y. L., Staudt, N., Tada, M., Ahrendt, R., Kazanskaya, O., Niehrs, C. and Houart, C. (2007). Dickkopf-1 regulates gastrulation movements by coordinated modulation of Wnt/betacatenin and Wnt/PCP activities, through interaction with the Dally-like homolog Knypek. *Genes Dev.* **21**, 465-480.

Ciruna, B., Jenny, A., Lee, D., Mlodzik, M. and Schier, A. F. (2006). Planar cell polarity signalling couples cell division and morphogenesis during neurulation. *Nature* **439**, 220-224.

Clevers, H. (2006). Wnt/beta-catenin signaling in development and disease. *Cell* **127**, 469-480.

Cohen, M. M., Jr (2003). The hedgehog signaling network. *Am. J. Med. Genet. A* **123**, 5-28.

Darken, R. S., Scola, A. M., Rakeman, A. S., Das, G., Mlodzik, M. and Wilson, P. A. (2002). The planar polarity gene strabismus regulates convergent extension movements in Xenopus. *EMBO J.* **21**, 976-985.

Davidson, G., Wu, W., Shen, J., Bilic, J., Fenger, U., Stannek, P., Glinka, A. and Niehrs, C. (2005). Casein kinase 1 gamma couples Wnt receptor activation to cytoplasmic signal transduction. *Nature* **438**, 867-872.

Glinka, A., Wu, W., Delius, H., Monaghan, A. P., Blumenstock, C. and Niehrs, C. (1998). Dickkopf-1 is a member of a new family of secreted proteins and functions in head induction. *Nature* **391**, 357-362.

Goto, T. and Keller, R. (2002). The planar cell polarity gene strabismus regulates convergence and extension and neural fold closure in Xenopus. *Dev. Biol.* **247**, 165-181.

Habas, R., Kato, Y. and He, X. (2001). Wnt/Frizzled activation of Rho regulates vertebrate gastrulation and requires a novel Formin homology protein Daam1. *Cell* **107**, 843-854.

Hyodo-Miura, J., Yamamoto, T. S., Hyodo, A. C., Iemura, S., Kusakabe, M., Nishida, E., Natsume, T. and Ueno, N. (2006). XGAP, an ArfGAP, is required for polarized localization of PAR proteins and cell polarity in Xenopus gastrulation. *Dev. Cell* **11**, 69-79.

Itasaki, N., Jones, C. M., Mercurio, S., Rowe, A., Domingos, P. M., Smith, J. C. and Krumlauf, R. (2003). Wise, a context-dependent activator and inhibitor of Wnt signalling. *Development* **130**, 4295-4305.

Jenny, A. and Mlodzik, M. (2006). Planar cell polarity signaling: a common mechanism for cellular polarization. *Mt. Sinai J. Med.* **73**, 738-750.

Jones, C. and Chen, P. (2007). Planar cell polarity signaling in vertebrates. *BioEssays* **29**, 120-132.

Kao, K. R. and Elinson, R. P. (1988). The entire mesodermal mantle behaves as Spemann's organizer in dorsoanterior enhanced Xenopus laevis embryos. *Dev. Biol.* **127**, 64-77.

Keller, R. and Danilchik, M. (1988). Regional expression, pattern and timing of convergence and extension during gastrulation of *Xenopus laevis*. *Development* **103**, 193-209.

Keller, R., Davidson, L. A. and Shook, D. R. (2003). How we are shaped: the biomechanics of gastrulation. *Differentiation* **71**, 171-205.

Kinoshita, N., Iioka, H., Miyakoshi, A. and Ueno, N. (2003). PKC delta is essential for Dishevelled function in a noncanonical Wnt pathway that regulates Xenopus convergent extension movements. *Genes Dev.* **17**, 1663-1676.

Klein, T. J. and Mlodzik, M. (2005). Planar cell polarization: an emerging model points in the right direction. *Annu. Rev. Cell Dev. Biol.* **21**, 155-176.

Kuhl, M., Geis, K., Sheldahl, L. C., Pukrop, T., Moon, R. T. and Wedlich, D. (2001). Antagonistic regulation of convergent extension movements in Xenopus by Wnt/beta-catenin and Wnt/Ca^{2+} signaling. *Mech. Dev.* **106**, 61-76.

Kushner, P. D. (1984). A library of monoclonal antibodies to Torpedo cholinergic synaptosomes. *J. Neurochem.* **43**, 775-786.

Lane, M. C. and Keller, R. (1997). Microtubule disruption reveals that Spemann's organizer is subdivided into two domains by the vegetal alignment zone. *Development* **124**, 895-906.

Li, L., Yuan, H., Weaver, C. D., Mao, J., Farr, G. H., 3rd, Sussman, D. J., Jonkers, J., Kimelman, D. and Wu, D. (1999). Axin and Frat1 interact with dvl and GSK, bridging Dvl to GSK in Wnt-mediated regulation of LEF-1. *EMBO J.* **18**, 4233-4240.

Montcouquiol, M., Sans, N., Huss, D., Kach, J., Dickman, J. D., Forge, A., Rachel, R. A., Copeland, N. G., Jenkins, N. A., Bogani, D. et al. (2006). Asymmetric localization of Vangl2 and Fz3 indicate novel mechanisms for planar cell polarity in mammals. *J. Neurosci.* **26**, 5265-5275.

Nieuwkoop, P. D. and Faber, J. (1994). *Normal Table of Xenopus laevis (Daudin).* New York: Garland.

Peng, H. B. (1991). Solutions and Protocols. In *Xenopus laevis: Practical uses in Cell and Molecular Biology*. Vol. 36 (ed. B. K. Kay and H. B. Peng), pp. 657-662. San Diego: Academic Press.

Penzo-Mendez, A., Umbhauer, M., Djiane, A., Boucaut, J. C. and Riou, J. F. (2003). Activation of Gbetagamma signaling downstream of Wnt-11/Xfz7 regulates Cdc42 activity during Xenopus gastrulation. *Dev. Biol.* **257**, 302-314.

Peters, J. M., McKay, R. M., McKay, J. P. and Graff, J. M. (1999). Casein kinase I transduces Wnt signals. *Nature* **401**, 345-350.

Sater, A. K., Steinhardt, R. A. and Keller, R. (1993). Induction of neuronal differentiation by planar signals in Xenopus embryos. *Dev. Dyn.* **197**, 268-280.

Sawin, K. E., Mitchison, T. J. and Wordeman, L. G. (1992). Evidence for kinesin-related proteins in the mitotic apparatus using peptide antibodies. *J. Cell Sci.* **101**, 303-313.

Schwarz-Romond, T., Asbrand, C., Bakkers, J., Kuhl, M., Schaeffer, H. J., Huelsken, J., Behrens, J., Hammerschmidt, M. and Birchmeier, W. (2002). The ankyrin repeat protein Diversin recruits Casein kinase Iepsilon to the beta-catenin degradation complex and acts in both canonical Wnt and Wnt/JNK signaling. *Genes Dev.* **16**, 2073-2084.

Shih, J. and Keller, R. (1992a). Cell motility driving mediolateral intercalation in explants of *Xenopus laevis*. *Development* **116**, 901-914.

Shih, J. and Keller, R. (1992b). Patterns of cell motility in the organizer and dorsal mesoderm of *Xenopus laevis*. *Development* **116**, 915-930.

Simons, M., Gloy, J., Ganner, A., Bullerkotte, A., Bashkurov, M., Kronig, C., Schermer, B., Benzing, T., Cabello, O. A., Jenny, A. et al. (2005). Inversin, the gene product mutated in nephronophthisis type II, functions as a molecular switch between Wnt signaling pathways. *Nat. Genet.* **37**, 537-543.

Sokol, S. Y. (1996). Analysis of Dishevelled signalling pathways during Xenopus development. *Curr. Biol.* **6**, 1456-1467.

Symes, K. and Smith, J. C. (1987). Gastrulation movements provide an early marker of mesoderm induction in *Xenopus laevis*. *Development* **101**, 339-349.

Tahinci, E. and Symes, K. (2003). Distinct functions of Rho and Rac are required for convergent extension during Xenopus gastrulation. *Dev. Biol.* **259**, 318-335.

Takeuchi, M., Nakabayashi, J., Sakaguchi, T., Yamamoto, T. S., Takahashi, H., Takeda, H. and Ueno, N. (2003). The prickle-related gene in vertebrates is essential for gastrulation cell movements. *Curr. Biol.* **13**, 674-679.

Tamai, K., Semenov, M., Kato, Y., Spokony, R., Liu, C., Katsuyama, Y., Hess, F., Saint-Jeannet, J. P. and He, X. (2000). LDL-receptor-related proteins in Wnt signal transduction. *Nature* **407**, 530-535.

Tamai, K., Zeng, X., Liu, C., Zhang, X., Harada, Y., Chang, Z. and He, X. (2004). A mechanism for Wnt coreceptor activation. *Mol. Cell* **13**, 149-156.

Tao, Q., Yokota, C., Puck, H., Kofron, M., Birsoy, B., Yan, D., Asashima, M., Wylie, C. C., Lin, X. and Heasman, J. (2005). Maternal wnt11 activates the canonical wnt signaling pathway required for axis formation in Xenopus embryos. *Cell* **120**, 857-871.

Ueno, N. and Greene, N. D. (2003). Planar cell polarity genes and neural tube closure. *Birth Defects Res. C Embryo Today* **69**, 318-324.

Wallingford, J. B. and Harland, R. M. (2001). *Xenopus* Dishevelled signaling regulates both neural and mesodermal convergent extension: parallel forces elongating the body axis. *Development* **128**, 2581-2592.

Wang, J., Mark, S., Zhang, X., Qian, D., Yoo, S. J., Radde-Gallwitz, K., Zhang, Y., Lin, X., Collazo, A., Wynshaw-Boris, A. et al. (2005). Regulation of polarized extension and planar cell polarity in the cochlea by the vertebrate PCP pathway. *Nat. Genet.* **37**, 980-985.

Wehrli, M., Dougan, S. T., Caldwell, K., O'Keefe, L., Schwartz, S., Vaizel-Ohayon, D., Schejter, E., Tomlinson, A. and DiNardo, S. (2000). arrow encodes an LDL-receptor-related protein essential for Wingless signalling. *Nature* **407**, 527-530.

Winklbauer, R. and Nagel, M. (1991). Directional mesoderm cell migration in the *Xenopus* gastrula. *Dev. Biol.* **148**, 573-589.

Yamanaka, H., Moriguchi, T., Masuyama, N., Kusakabe, M., Hanafusa, H., Takada, R., Takada, S. and Nishida, E. (2002). JNK functions in the non-canonical Wnt pathway to regulate convergent extension movements in vertebrates. *EMBO Rep.* **3**, 69-75.

Yan, D., Wallingford, J. B., Sun, T. Q., Nelson, A. M., Sakanaka, C., Reinhard, C., Harland, R. M., Fantl, W. J. and Williams, L. T. (2001). Cell autonomous regulation of multiple Dishevelled-dependent pathways by mammalian Nkd. *Proc. Natl. Acad. Sci. USA* **98**, 3802-3807.

Yanagawa, S., van Leeuwen, F., Wodarz, A., Klingensmith, J. and Nusse, R. (1995). The dishevelled protein is modified by wingless signaling in Drosophila. *Genes Dev.* **9**, 1087-1097.
Yokota, C., Kofron, M., Zuck, M., Houston, D. W., Isaacs, H., Asashima, M., Wylie, C. C. and Heasman, J. (2003). A novel role for a nodal-related protein; Xnr3 regulates convergent extension movements via the FGF receptor. *Development* **130**, 2199-2212.
Zeng, X., Tamai, K., Doble, B., Li, S., Huang, H., Habas, R., Okamura, H., Woodgett, J. and He, X. (2005). A dual-kinase mechanism for Wnt co-receptor phosphorylation and activation. *Nature* **438**, 873-877.